Thymic progenitors of TCRαβ$^+$ CD8αα intestinal intraepithelial lymphocytes require RasGRP1 for development

Dominic P. Golec,[1] Romy E. Hoeppli,[2] Laura M. Henao Caviedes,[1] Jillian McCann,[1] Megan K. Levings,[2] and Troy A. Baldwin[1]

[1]Department of Medical Microbiology and Immunology, University of Alberta, Edmonton, AB, Canada
[2]Department of Surgery, University of British Columbia, Vancouver, BC, Canada

Strong T cell receptor (TCR) signaling largely induces cell death during thymocyte development, whereas weak TCR signals induce positive selection. However, some T cell lineages require strong TCR signals for differentiation through a process termed agonist selection. The signaling relationships that underlie these three fates are unknown. RasGRP1 is a Ras activator required to transmit weak TCR signals leading to positive selection. Here, we report that, despite being dispensable for thymocyte clonal deletion, RasGRP1 is critical for agonist selection of TCRαβ$^+$CD8αα intraepithelial lymphocyte (IEL) progenitors (IELps), even though both outcomes require strong TCR signaling. Bim deficiency rescued IELp development in RasGRP1$^{-/-}$ mice, suggesting that RasGRP1 functions to promote survival during IELp generation. Additionally, expression of CD122 and the adhesion molecules $\alpha_4\beta_7$ and CD103 define distinct IELp subsets with differing abilities to generate TCRαβ$^+$CD8αα IEL in vivo. These findings demonstrate that RasGRP1-dependent signaling underpins thymic selection processes induced by both weak and strong TCR signals and is differentially required for fate decisions derived from a strong TCR stimulus.

INTRODUCTION

The affinity of TCR:self-peptide-MHC interactions is a key determinant of thymocyte fate (Klein et al., 2014). Relatively low-affinity self-peptide-MHC stimulation through the TCR drives thymocyte positive selection, resulting in the development of conventional CD4$^+$ and CD8$^+$ T cells. Generally, high-affinity TCR stimulation results in clonal deletion and removal of thymocytes with self-reactive TCRs from the T cell repertoire. However, more recently, it has been appreciated that high-affinity, or agonist, stimulation through the TCR is required for positive selection of several alternatively selected thymocyte lineages. This process has been termed "agonist selection" and instructs the development of numerous nonconventional T cell lineages such as invariant NKT cells (iNKT), thymic regulatory T cells (tTreg), and natural T_H17 cells (nT_H17) within the thymus (Stritesky et al., 2012). In addition, agonist selection guides the development of progenitor cells that give rise to a subset of intestinal TCRαβ$^+$ intraepithelial lymphocytes (IELs) characterized by their unique expression of unconventional CD8αα homodimers (TCRαβ$^+$CD8αα IELs). Although the requirement for high-affinity TCR signaling to drive agonist selection and clonal deletion has been well defined, the nature of the signals that differentiate these two opposing processes remain unclear.

The intestinal epithelium contains distinct populations of IELs that are thought to regulate intestinal homeostasis and whose dysregulation has been implicated in numerous disease models (Cheroutre et al., 2011). Intestinal IELs are heterogeneous, reflecting their distinct developmental origins. Broadly, the intestinal IEL pool includes both γδ– and αβ–T cell lineages. TCRαβ$^+$ IEL can be further classified into "natural" and "induced" subsets (Cheroutre et al., 2011). Induced IELs arise from mature naive CD4$^+$ or CD8$^+$ T cells after peripheral activation. Natural IELs are generated from thymic precursors that migrate to the intestine where they complete their development. Furthermore, natural IELs are characterized by expression of CD8αα homodimers but not CD8αβ heterodimers. Local IL-15 signals induce expression of the transcription factor T-bet and the CD8αα homodimer (Lai et al., 2008; Ma et al., 2009; Klose et al., 2014; Reis et al., 2014). Historically, the identity of the thymic precursor of TCRαβ$^+$CD8αα IELs has been contentious. Although early work suggested preselection double-negative (DN) thymocytes as the direct IEL precursor, more recent studies have conclusively shown IEL progenitors (IELps) arise from double-positive (DP) thymocytes after a high-affinity TCR signal (Leishman et al., 2002; Eberl and Littman, 2004; Gangadharan et al., 2006). Part of the confusion likely stemmed from the fact that after a high-affinity TCR signal, DP thymocytes

Correspondence to Troy A. Baldwin: tbaldwin@ualberta.ca

Abbreviations used: DN, double negative; DP, double positive; ERK, extracellular signal-regulated kinase; IEL, intraepithelial lymphocyte; IELp, IEL progenitor; iNKT cell, invariant NKT cell; MFI, mean fluorescence intensity; SP, single positive; tTreg cell, thymic regulatory T cell.

The Rockefeller University Press
J. Exp. Med. 2017 Vol. 214 No. 8 2421–2435
https://doi.org/10.1084/jem.20170844

down-regulate expression of CD4 and CD8 and IELp cells reside within the DP^{dull} and DN thymocyte fractions (Gangadharan et al., 2006; McDonald et al., 2014). Within this DN + DP^{dull} population, IELp cells display high expression of TCRβ and CD5, but only a fraction of this population expresses markers of high-affinity Ag encounter, such as CD122, PD-1, and Helios (Hanke et al., 1994; Gangadharan et al., 2006; Klose et al., 2014; McDonald et al., 2014). Whether the entire $TCR\beta^+CD5^+$ population, or only a subfraction thereof, is truly an IELp is unclear. IELp cells are also thought to up-regulate expression of gut-homing molecules like the chemokine receptor CCR9 (Zabel et al., 1999; Mora et al., 2003) and the integrins $\alpha_4\beta_7$ and CD103 within the thymus (Andrew et al., 1996; Guo et al., 2015). Although we are beginning to learn more about the phenotypic characteristics of IELps, the signaling events controlling IELp generation in the thymus are not well understood.

Perhaps the best-defined feature of the IELp population is their expression of self-reactive TCRs. Early work demonstrated an enrichment of "forbidden" superantigen reactive Vβ clones within the $TCR\alpha\beta^+CD8\alpha\alpha$ IEL compartment, indicating that signals that would normally result in thymic clonal deletion promoted the development of this population (Rocha et al., 1991; Poussier et al., 1992). Consistent with high-affinity signals driving both clonal deletion and agonist selection, thymocytes impaired in cell death pathways show dramatically increased numbers of IELp cells and $TCR\alpha\beta^+$ CD8αα IELs (Pobezinsky et al., 2012; McDonald et al., 2014). This increase likely occurs as a result of impaired thymocyte clonal deletion. TGFβ signaling also promotes agonist selection as $TGF\beta1^{-/-}$ and $TGF\beta RI^{-/-}$ mice lack IELp cells and intestinal $TCR\alpha\beta^+CD8\alpha\alpha$ IELs (Konkel et al., 2011), possibly because of curbing clonal deletion rather than providing an inductive signal (Ouyang et al., 2010). Finally, thymocytes lacking CD28 costimulatory signals show large increases in numbers of IELp cells and $TCR\alpha\beta^+CD8\alpha\alpha$ IELs, as the result of clonal diversion of cells normally destined for clonal deletion into the IEL lineage (Pobezinsky et al., 2012). Collectively, these data support an intimate relationship between the signals that induce clonal deletion and those that promote agonist selection.

Although there is relatively abundant information regarding the molecular mechanisms that regulate positive and negative selection, there is limited information regarding the pathways that differentiate clonal deletion from agonist selection. Furthermore, whether signals that drive conventional positive selection are also required for agonist selection is unclear. One pathway that has long been shown to be differentially involved in positive selection and clonal deletion is the Ras–extracellular signal-regulated kinase (Erk) pathway. Although Erk is not required for clonal deletion (McGargill et al., 2009), high-affinity TCR signaling induces a transient burst of high-intensity Erk activation (Werlen et al., 2003; Daniels et al., 2006). In contrast, positive selection requires sustained Erk activation (McNeil et al., 2005; Daniels et al., 2006). This paradigm is reinforced through analysis of mice lacking RasGRP1, a positive regulator of Ras–Erk signaling in DP thymocytes (Dower et al., 2000; Priatel et al., 2002). Thymocytes from RasGRP1-deficient mice display a block in positive selection, but appear to undergo clonal deletion normally, suggesting that RasGRP1 specifically regulates the duration of Erk activation (Priatel et al., 2002; Kortum et al., 2012). With respect to the relationship between positive selection, clonal deletion and agonist selection, the connecting peptide motif within the TCRα chain (α-CPM) was previously shown to be required for positive selection by regulating Erk activation (Bäckström et al., 1998; Werlen et al., 2000). The α-CPM is also required for agonist selection, but mutation of the α-CPM does not impact clonal deletion (Leishman et al., 2002). In contrast, it was recently shown that Themis, a molecule important for regulating TCR signal strength and downstream Erk activation leading to positive selection, is not required for either clonal deletion or agonist selection (Lesourne et al., 2012; Fu et al., 2013). Of note, the role of RasGRP1 in the generation of $TCR\alpha\beta^+CD8\alpha\alpha$ gut IELs has not been investigated. Therefore, although the Ras–Erk pathway is a central discriminator of thymocyte fate during positive selection and clonal deletion, its role and regulation in agonist selection is less clear.

To gain insight into the relationship between positive selection, clonal deletion and agonist selection and the potential role of the Ras–Erk pathway in regulating these fates, we examined thymocyte selection in mice lacking RasGRP1. We observed markedly reduced numbers of both $TCR\alpha\beta^+$ CD8αα IEL and IELp cells in RasGRP1-deficient mice. Furthermore, of the RasGRP1-deficient IELps that were present, most showed impaired expression of markers of high-affinity antigen encounter. Genetic deletion of the pro-apoptotic protein Bim on the RasGRP1-deficient background rescued the development of IELps, including the percentage of cells that had received a strong TCR signal, suggesting that RasGRP1 is required to transmit survival signals during IELp selection. In addition, we found distinct IELp subsets that varied with respect to cell surface phenotype, age after selection, and ability to generate $TCR\alpha\beta^+CD8\alpha\alpha$ IELs in vivo. These results provide novel insight into the TCR signaling events that guide agonist selection of IELp cells and highlight the functional heterogeneity of this subset.

RESULTS

RasGRP1 regulates $TCR\alpha\beta^+CD8\alpha\alpha$ IEL development through control of IELp generation

To investigate a potential role for RasGRP1 in $TCR\alpha\beta^+$ CD8αα IEL generation, we examined IEL populations present in small intestines from WT and RasGRP1 KO (1KO) mice. Within the $CD45^+CD4^-$ compartment, 1KO mice showed significantly reduced frequencies and numbers of $TCR\alpha\beta^+$ CD8αα IELs relative to WT mice (Fig. 1, A and B). Additionally, greater frequencies and numbers of $TCR\gamma\delta^+CD8\alpha\alpha$ were isolated from 1KO mice relative to WT, suggesting that

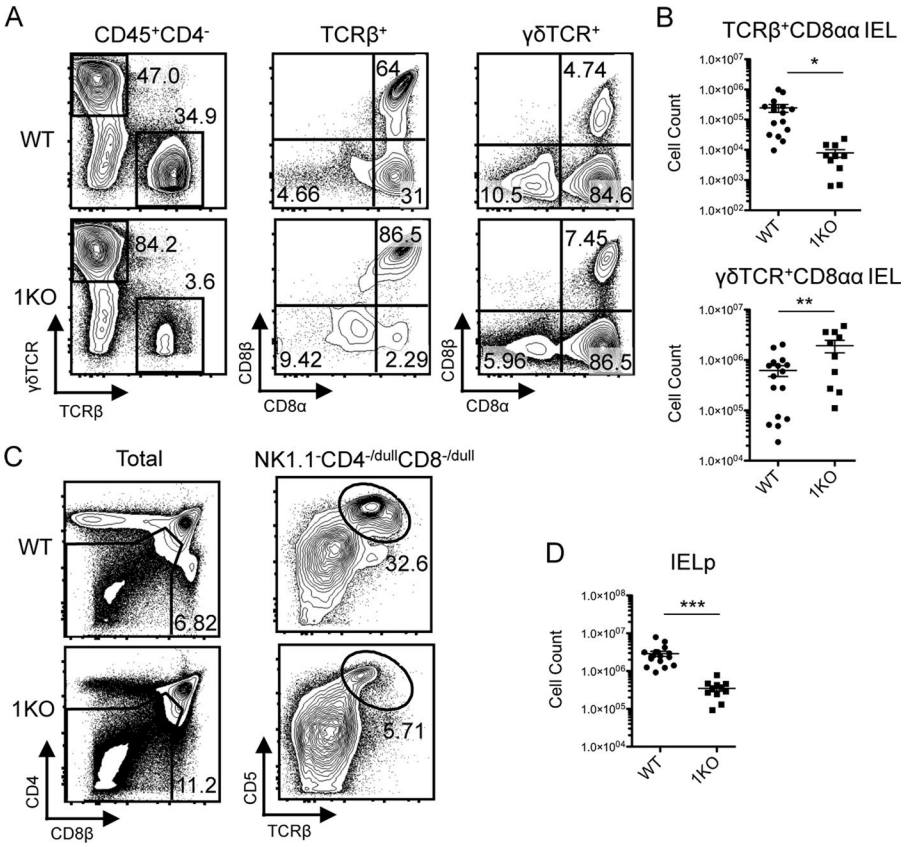

Figure 1. **RasGRP1 is required for efficient TCRαβ$^+$ CD8αα IEL development through control of thymic IELp generation.** IELs were isolated from small intestines of WT and 1KO animals and analyzed by flow cytometry. (A) CD45$^+$CD4$^-$ cells were gated and analyzed for expression of TCRβ and TCRγδ (left). TCRβ$^+$ (middle) and γδTCR$^+$ (right) IELs were analyzed for expression of CD8α and CD8β. (B) Numbers of TCRαβ$^+$ CD8αα IELs (top) and γδTCR$^+$CD8αα (bottom) isolated from the indicated mice. Data were obtained from the indicated number of mice over 14 individual experiments; WT (n = 16), 1KO (n = 10). (C) Thymi were harvested from the indicated mice and analyzed for the presence of IELp cells. Total thymocytes were analyzed for expression of CD4 and CD8 and CD4$^{-/dull}$CD8$^{-/dull}$ were gated (left). NK1.1$^-$ cells were subsequently analyzed for expression of TCRβ and CD5 (right). (D) Number of IELp cells (CD4$^{-/dull}$CD8$^{-/dull}$NK1.1$^-$TCRβ$^+$CD5$^+$) from the indicated mice. Data were obtained from the indicated number of mice over 17 individual experiments; WT (n = 17), 1KO (n = 11). *, P < 0.05; **, P < 0.01; ***, P < 0.001 (unpaired Student's t test). Error bars indicate SEM.

RasGRP1 is not required for TCRγδ$^+$CD8αα IEL development (Fig. 1, A and B).

Because thymic progenitors are known to give rise to TCRαβ$^+$CD8αα IELs, we examined thymocytes from WT and 1KO mice for the presence of IELps. Based on several previous studies (Gangadharan et al., 2006; Klose et al., 2014; McDonald et al., 2014), we identified IELp cells as having a CD4$^{-/dull}$CD8$^{-/dull}$NK1.1$^-$TCRβ$^+$CD5$^+$ phenotype (Fig. 1 C). Compared with WT mice, 1KO mice contained higher frequencies of CD4$^{-/dull}$CD8$^{-/dull}$ thymocytes, but fewer of these cells were NK1.1$^-$TCRβ$^+$CD5$^+$. Similar to the pattern observed in TCRαβ$^+$CD8αα IELs, 1KO thymi showed significantly reduced numbers of IELps compared with WT (Fig. 1 D). Collectively, these data suggest that RasGRP1 regulates TCRαβ$^+$CD8αα IEL generation through promoting the development of thymic IELp cells.

RasGRP1-deficient IELp cells show signs of impaired TCR signaling

Signaling through CD122, expressed on the cell surface of IELp cells that have reached the small intestine, is required for the IL-15–dependent generation of TCRαβ$^+$CD8αα IELs within the gut. Furthermore, CD122 has been shown to be up-regulated after high-affinity antigen encounter in the thymus and is expressed on the surface of a fraction of IELp cells within the thymus (Hanke et al., 1994). Therefore, we wished to determine whether RasGRP1 influenced the frequency of IELps that express CD122. Despite finding markedly reduced numbers of IELps in 1KO thymi, we observed similar frequencies of CD122$^-$ and CD122$^+$ IELps within WT and 1KO animals (Fig. 2 A and Fig. S1 A). Given that we observed two distinct populations of IELps based on expression of CD122, we divided the IELp population into CD122$^-$ and CD122$^+$ fractions for subsequent analysis of IELp development.

Because IELps are generated after strong TCR signaling (McDonald et al., 2014) and RasGRP1 is a key regulator of TCR signaling at various stages of thymocyte development (Priatel et al., 2002; Shen et al., 2011; Golec et al., 2013), we examined the expression of proteins regulated by strong TCR signals. Both the co-inhibitory molecule PD-1 and transcription factor Helios are induced after high-affinity TCR signaling (Baldwin and Hogquist, 2007; Daley et al., 2013). In both WT and 1KO IELps, we observed significantly increased frequencies of PD-1$^+$Helios$^+$ cells within CD122$^+$ IELps compared with CD122$^-$ IELps, suggesting that high-affinity signaled IELps were enriched within the CD122$^+$ fraction. However, there was a significant reduction in the frequency of PD-1$^+$Helios$^+$ cells in 1KO mice compared with WT mice in both the CD122$^-$ and CD122$^+$ IELp fractions (Fig. 2, B and C). Collectively, these data suggest that RasGRP1 deficiency impairs the generation of high-affinity signaled IELps.

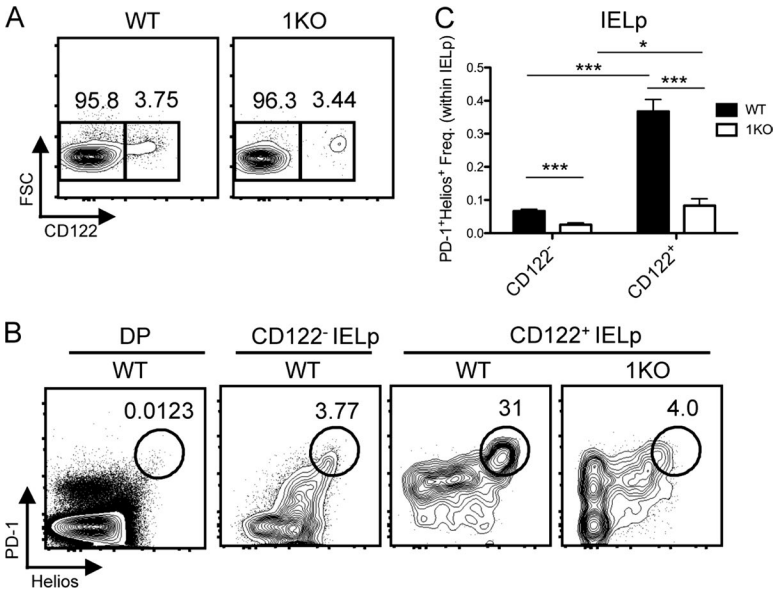

Figure 2. **IELps from RasGRP1-deficient animals show signs of impaired TCR signaling.** (A) Representative expression of CD122 on IELp cells ($CD4^{-/dull}CD8^{-/dull}$ $NK1.1^{-}TCR\beta^{+}CD5^{+}$) from WT and 1KO mice. Data were obtained from the indicated number of mice over 17 individual experiments; WT (n = 17), 1KO (n = 11). (B) Representative PD-1 and Helios expression on DP thymocytes and $CD122^{-}$ IELp from WT mice and $CD122^{+}$ IELp cells from WT and 1KO mice. (C) Frequencies of $PD\text{-}1^{+}Helios^{+}$ cells within $CD122^{-}$ and $CD122^{+}$ IELp cells from the indicated mice. Data were obtained from the indicated number of mice over nine individual experiments; WT (n = 9), 1KO (n = 5). *, $P < 0.05$; ***, $P < 0.001$ (unpaired Student's t test). Error bars indicate SEM.

RasGRP1 is dispensable for thymocyte clonal deletion but is required for positive selection and transmission of high-affinity TCR signals

To further dissect the involvement of RasGRP1 during thymic selection events, we crossed RasGRP1-deficient mice to the physiological HY^{cd4} TCR transgenic mouse model to allow examination of thymocytes with a fixed TCR specificity (Baldwin et al., 2005). HY^{cd4} mice express an MHCI-restricted, male Ag–specific TCR that is recognized by the mAb T3.70. Female HY^{cd4} mice are a model of positive selection because of a lack of high-affinity Ag expression, whereas male mice provide a model to examine responses to high affinity peptide. As expected from a previous study (Priatel et al., 2002), HY^{cd4} female mice showed a robust Ag-specific ($T3.70^{+}$) CD8SP thymocyte population, which was severely reduced in the absence of RasGRP1 (Fig. 3 A). Thymocytes from HY^{cd4} $RasGRP1^{-/-}$ male mice showed a similar reduction of Ag-specific CD8SP thymocytes compared with their RasGRP1-sufficient counterparts, suggesting that clonal deletion remains intact in the absence of RasGRP1. To directly evaluate clonal deletion, we examined caspase 3 activation within male HY^{cd4} and HY^{cd4} $RasGRP1^{-/-}$ $T3.70^{+}$ thymocytes. Although $T3.70^{+}$ DP^{bright} thymocytes showed little caspase 3 activation in both HY^{cd4} and HY^{cd4} $RasGRP1^{-/-}$ male mice, $T3.70^{+}$ DP^{dull} thymocytes from both strains showed similar, elevated percentages of active caspase 3^{+} cells (Fig. 3 B). These data confirm that although RasGRP1 is required for positive selection, it is dispensable for thymocyte clonal deletion, as has been reported previously using conventional TCR transgenic models (Priatel et al., 2002).

We next evaluated the impact of RasGRP1 deficiency on high-affinity TCR signaling in vivo using the HY^{cd4} TCR transgenic model. As conventional TCR transgenic mice expressing high-affinity Ag largely lack a DP thymocyte population, the use of the HY^{cd4} model allows the examination of RasGRP1-dependent signaling in DP thymocytes in vivo. As expected, we observed higher frequencies of $PD\text{-}1^{+}Helios^{+}$ thymocytes in $T3.70^{+}$ DP^{dull} compared with DP^{bright} populations in HY^{cd4} male mice (Fig. 3 C; Hu and Baldwin, 2015). However, $T3.70^{+}$ DP^{bright} and DP^{dull} fractions from HY^{cd4} $RasGRP1^{-/-}$ male mice showed few $PD\text{-}1^{+}Helios^{+}$ cells (Fig. 3 C). Additionally, we examined the $CD4^{-/dull}CD8^{-/dull}$ compartment of HY^{cd4} male mice to examine the expression of other proteins induced by strong TCR signaling. We found a prominent population of $T3.70^{+}CD5^{+}$ thymocytes within the $CD4^{-/dull}CD8^{-/dull}$ population that was substantially reduced in HY^{cd4} $RasGRP1^{-/-}$ male mice (Fig. 3 D). Furthermore, within the $CD4^{-/dull}CD8^{-/dull}T3.70^{+}CD5^{+}$ thymocyte compartment, HY^{cd4} $RasGRP1^{-/-}$ male mice showed reduced frequencies of $CD122^{+}$ cells relative to their WT counterparts (Fig. 3 D and Fig. S1 B), which was different than what was observed with polyclonal mice. Altogether, these results demonstrate that RasGRP1-deficient thymocytes show reduced expression of multiple markers of strong TCR signaling, suggesting that RasGRP1 regulates TCR signaling strength after high-affinity antigen encounter.

Bim deletion rescues the generation of IELps in RasGRP1-deficient mice

Either impairment in the transmission of differentiation signals required for selection and/or an inability of IELps to survive could underlie the defect in IELp generation in 1KO mice. To determine whether increased apoptosis caused the defect in IELp generation, we intercrossed $RasGRP1^{-/-}$ and $Bim^{-/-}$ (BKO) mice to create $RasGRP1^{-/-}$ $Bim^{-/-}$ double KO (DKO) mice. As previously reported, BKO thymocytes were impaired in apoptosis induction and display enhanced selection of IELps (McDonald et al., 2014) compared with WT (Fig. 4, A and B). Deletion of Bim in the 1KO background resulted in the generation of IELps to levels above WT, but

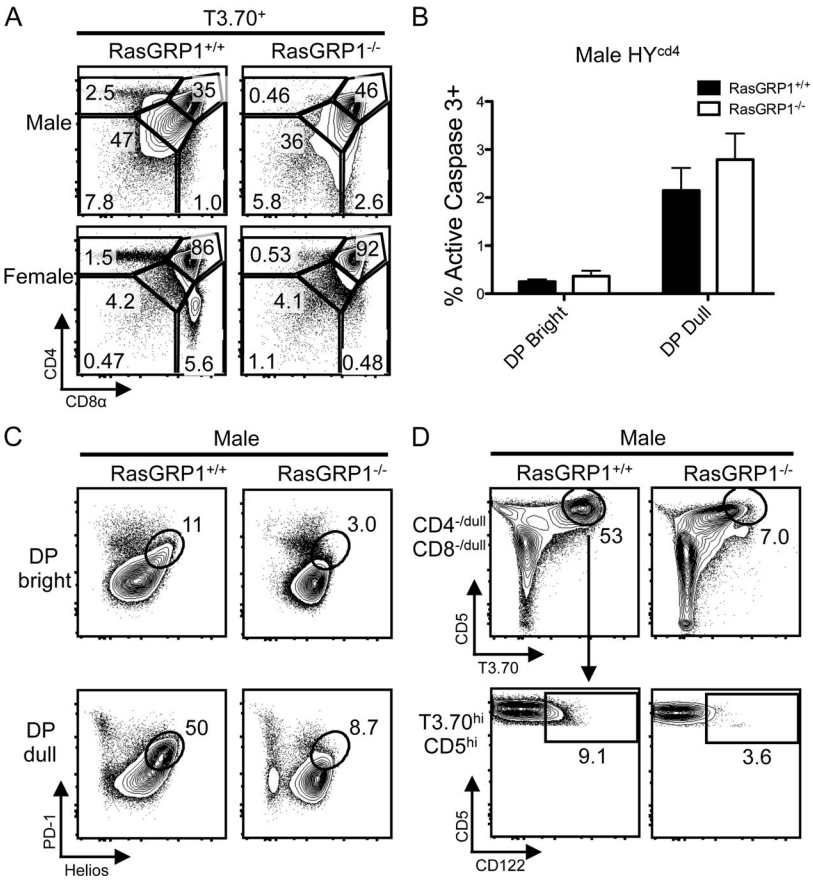

Figure 3. **RasGRP1 is dispensable for thymocyte clonal deletion but is required for positive selection and regulates the expression of molecules induced by high-affinity TCR stimulation.** HY^{cd4} mice were crossed onto the RasGRP1 KO background, and thymi from male and female HY^{cd4} animals were examined. (A) CD4 and CD8 profiles of T3.70$^+$ thymocytes from the indicated mice. (B) Percentages of active caspase 3$^+$ T3.70$^+$ DP^{bright} and DP^{dull} cells. Error bars indicate SEM. (C) PD-1 and Helios profiles of T3.70$^+$ DP^{bright} and DP^{dull} cells from the indicated mice. (D) CD4$^{-/dull}$CD8$^{-/dull}$ cells from the indicated mice were examined for expression of CD5 and T3.70 (top). T3.70^{hi}CD5^{hi} thymocytes were analyzed for expression of CD5 and CD122 (bottom). Data in A–C are representative of four individual experiments; $n = 4$. D is representative of three individual experiments; $n = 3$.

below BKO mice (Fig. 4, A and B). There was no change in the frequency of CD122$^+$ IELps in DKO compared with WT mice, but a rescue in the frequency of PD-1$^+$Helios$^+$ cells within the CD122$^+$ fraction (Fig. 4, C and D; and Fig. S1 A). DKO mice contained a similar number of TCR$\alpha\beta^+$CD8$\alpha\alpha$ IELs as WT, indicating that 1KO IELps rescued from apoptosis by Bim deficiency could give rise to TCR$\alpha\beta^+$CD8$\alpha\alpha$ IELs (Fig. S2). Examination of apoptosis directly ex vivo through active caspase 3 staining revealed consistently higher levels of apoptosis in 1KO IELps in both CD122$^-$ and CD122$^+$ fractions compared with WT, but this was not statistically significant (Fig. 4 E). However, it is important to note that the transition from CD122$^-$ to CD122$^+$ resulted in a statistically significant decrease in the frequency of active caspase 3$^+$ cells in both WT and 1KO mice, suggesting that CD122$^+$ IELps are protected from apoptosis (Fig. 4 E).

Heterogeneity within the IELp population is highlighted by differences in expression of adhesion molecules and proteins regulated by TCR signal strength

Given the impact of RasGRP1 deficiency on the number of intestinal TCR$\alpha\beta^+$CD8$\alpha\alpha$ IELs appeared greater (~30-fold) than on the number of thymic IELps (~10-fold), we hypothesized that RasGRP1 may further regulate specific subsets of thymic IELps that could give rise to TCR$\alpha\beta^+$ CD8$\alpha\alpha$ IELs. Therefore, we examined IELp cells for the expression of adhesion molecules $\alpha_4\beta_7$ and CD103 because both integrins have been shown to be induced on IELps within the thymus and may regulate progenitor migration to the gut (Andrew et al., 1996; Guo et al., 2015). Most CD122$^-$ IELp cells did not express either $\alpha_4\beta_7$ or CD103 (Fig. 5 A). In contrast, CD122$^+$ IELps contained four distinct populations of $\alpha_4\beta_7$- and CD103-expressing cells, with the $\alpha_4\beta_7^-$CD103$^-$, $\alpha_4\beta_7^+$CD103$^-$, and $\alpha_4\beta_7^-$CD103$^+$ populations being most prominent and $\alpha_4\beta_7^+$CD103$^+$ cells constituting a minor fraction (Fig. 5 A). To determine whether the absence of RasGRP1 and/or Bim regulated these IELp subsets, we examined adhesion molecule expression on CD122$^+$ IELps from 1KO and BKO mice. RasGRP1-deficient CD122$^+$ IELps showed increased frequencies, but reduced numbers of the $\alpha_4\beta_7^-$CD103$^-$ subset, and reduced frequencies and numbers of all other subsets, relative to WT (Fig. 5, A and B). In contrast, BKO IELps showed significantly increased frequencies and numbers of $\alpha_4\beta_7^+$CD103$^-$ cells relative to WT and reduced frequencies, but similar numbers, of $\alpha_4\beta_7^-$CD103$^+$ IELps (Fig. 5, A and B). Collectively, these results suggest the composition of the CD122$^+$ IELp pool is altered in 1KO and BKO thymi, which may account for altered TCR$\alpha\beta^+$CD8$\alpha\alpha$ IEL development in these animals.

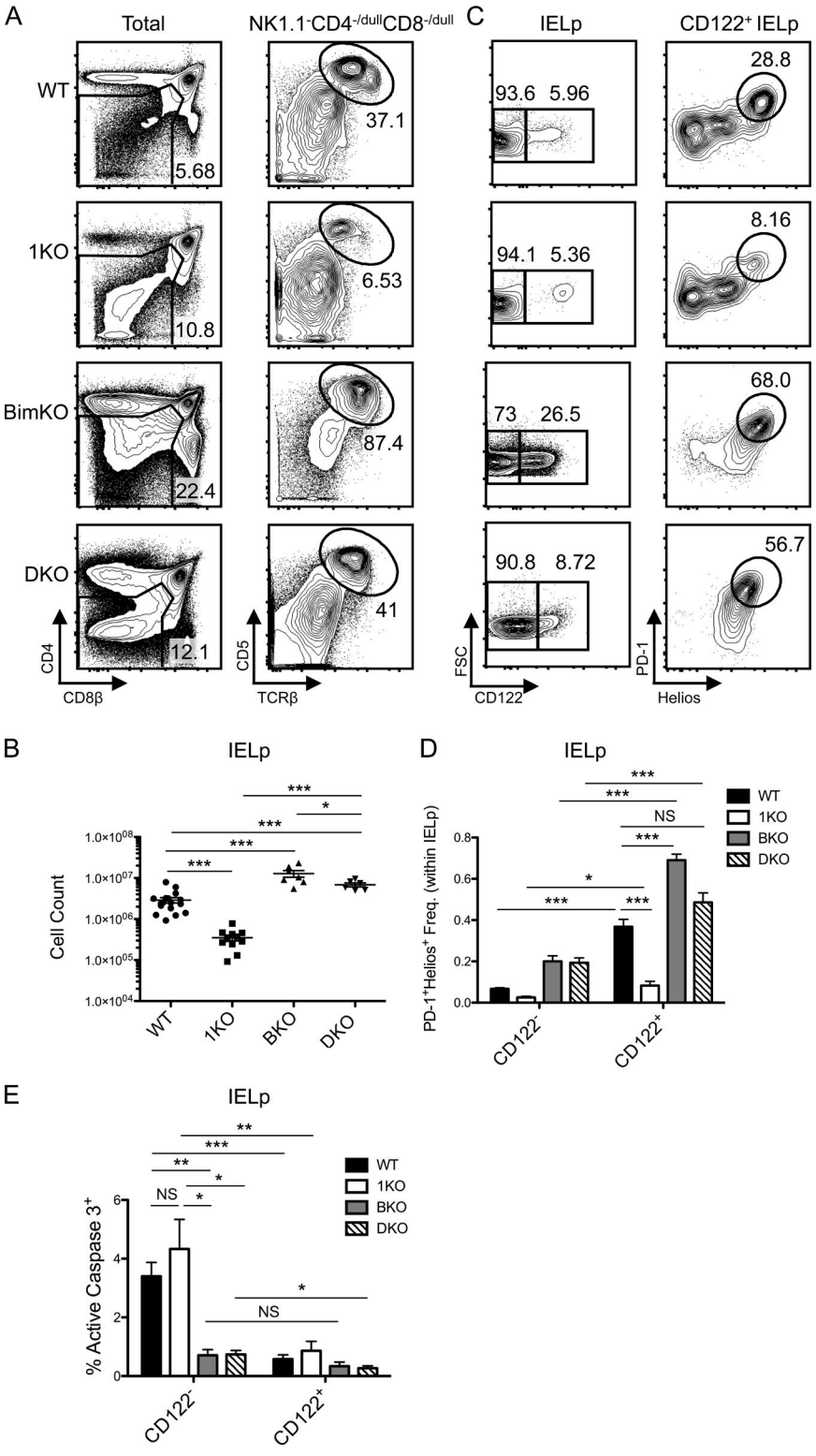

Figure 4. **Bim deletion rescues the generation of IELps in RasGRP1-deficient mice.** RasGRP1$^{-/-}$ mice were crossed onto the Bim$^{-/-}$ background to create DKO mice. (A) Thymi were harvested from the indicated mice and analyzed for the presence of IELp cells. Total thymocytes were analyzed for expression of CD4 and CD8 and CD4$^{-/dull}$CD8$^{-/dull}$ were gated (left). NK1.1^{-} cells were subsequently analyzed for expression of TCRβ and CD5 (right). (B) Number of IELp cells (CD4$^{-/dull}$CD8$^{-/dull}$NK1.1^{-}TCRβ^{+}CD5^{+}) from the indicated mice. Data were obtained from the indicated number of mice over 17 individual experiments; WT (n = 17), 1KO (n = 11), BKO (n = 7), DKO (n = 6). (C) Representative expression of CD122 on IELp cells (CD4$^{-/dull}$CD8$^{-/dull}$NK1.1^{-}TCRβ^{+}CD5^{+}; left) and representative PD-1 and Helios expression on CD122^{+} IELp cells (right) from the indicated mice. (D) Frequencies of PD-1^{+}Helios^{+} cells within CD122^{-} and CD122^{+} IELp fractions from the indicated mice. Data were obtained from the indicated number of mice over nine individual experiments; WT (n = 9), 1KO (n = 5), BKO (n = 5), DKO (n = 6). (E) Percentages of active caspase 3^{+} cells within the CD122^{-} and CD122^{+} IELp fractions from the indicated mice. Data were obtained from the indicated number of mice over 12 individual experiments; WT (n = 11), 1KO (n = 8), BKO (n = 4), DKO (n = 6). *, P < 0.05; **, P < 0.01; ***, P < 0.001 (unpaired Student's t test). Error bars indicate SEM.

Because we observed significant differences in $\alpha_4\beta_7$ and CD103 expression between CD122^{-} and CD122^{+} IELps and within the different strains of mice, we further analyzed these distinct fractions to gain insight into the relationship between TCR signaling and adhesion molecule expression in these cells. To examine the strength of TCR signaling in CD122^{-} and CD122^{+} IELp cells, we used the Nur77^{GFP} reporter mouse (Moran et al., 2011). Levels of Nur77 expression downstream

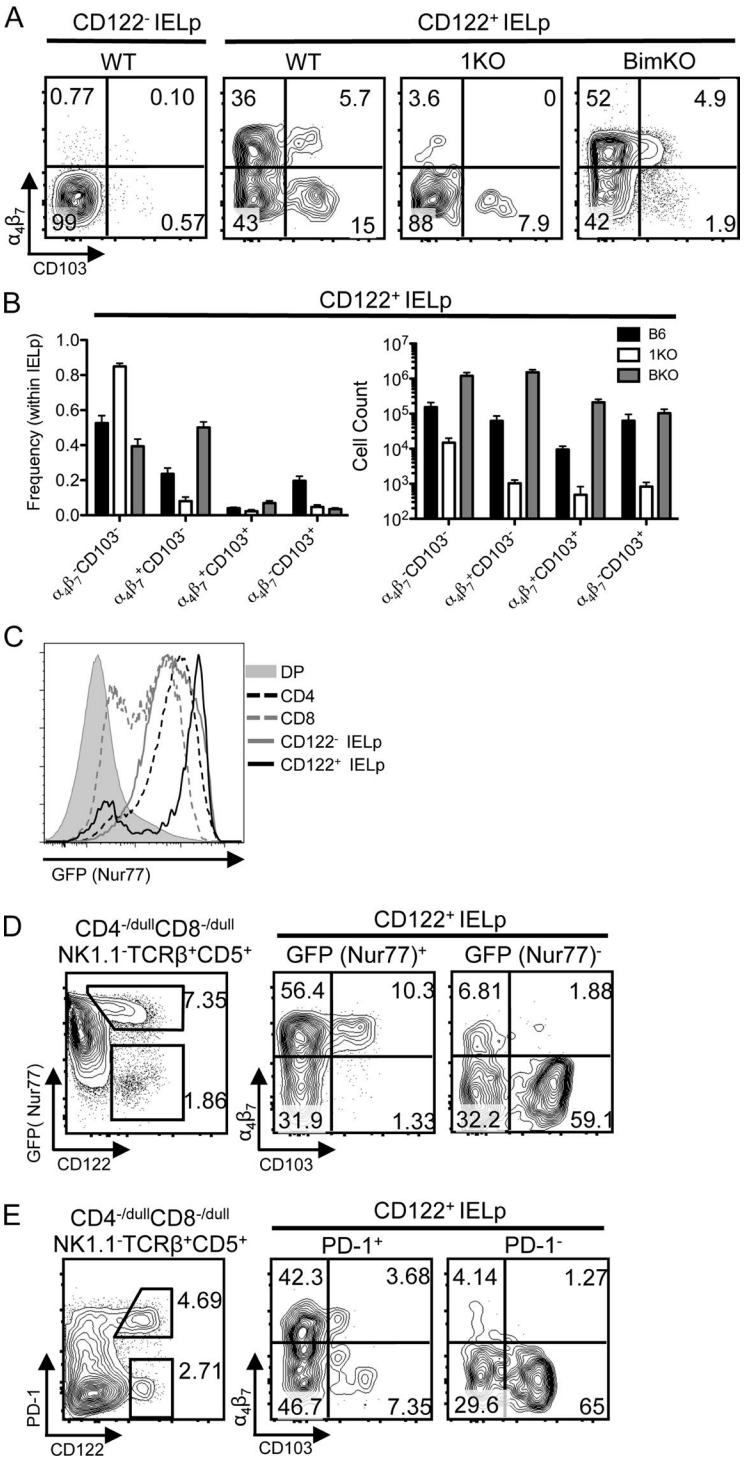

Figure 5. **IELp cells showing signs of recent high-affinity TCR signaling display increased expression of $\alpha_4\beta_7$, whereas IELp cells lacking signs of high-affinity TCR signals are skewed toward expression of CD103.** Thymocytes were analyzed for markers TCR signaling strength and the adhesion molecules $\alpha_4\beta_7$ and CD103 to dissect the heterogeneity of the IELp ($CD4^{-/dull}CD8^{-/dull}NK1.1^{-}TCR\beta^{+}CD5^{+}$) population. (A) $CD122^{-}$ and $CD122^{+}$ IELp cells from the indicated mice were analyzed for expression of $\alpha_4\beta_7$ and CD103. Data are representative of six individual experiments; WT ($n = 6$), 1KO ($n = 6$), BKO ($n = 6$). (B) Frequencies (left) and numbers (right) of $\alpha_4\beta_7$- and CD103-expressing subpopulations of $CD122^{+}$ IELps. Error bars indicate SEM. (C) GFP expression in DP, CD4SP, CD8SP, $CD122^{-}$ IELp, and $CD122^{+}$ IELp thymocyte populations from $Nur77^{GFP}$ reporter mice. Data are representative of five individual experiments; $n = 5$. (D) IELp cells were analyzed for expression of GFP and CD122. $GFP^{hi}CD122^{+}$ and $GFP^{lo}CD122^{+}$ thymocytes from $Nur77^{GFP}$ mice were subsequently examined for expression of $\alpha_4\beta_7$ and CD103 (right). Data are representative of five individual experiments; $n = 5$. (E) IELp cells were analyzed for expression of PD-1 and CD122 (left). $PD\text{-}1^{+}CD122^{+}$ and $PD\text{-}1^{-}CD122^{+}$ were examined for expression of $\alpha_4\beta_7$ and CD103 (right). Data are representative of four individual experiments; $n = 4$.

of TCR stimulation are proportional to the strength of TCR signaling experienced by thymocytes, making this a useful model for studying TCR signal strength. Similar to previously published data using $Nur77^{GFP}$ mice (Moran et al., 2011), we saw that both mature CD4SP and CD8SP thymocytes expressed increased levels of GFP relative to DP thymocytes, with CD4SP thymocytes displaying elevated levels of GFP compared with CD8SP thymocytes (Fig. 5 C). $CD122^{-}$ IELp cells showed a relatively uniform pattern of GFP expression that overlapped both CD4SP and CD8SP thymocytes. The $CD122^{+}$ IELp pool displayed a bimodal pattern of GFP expression, such that one fraction showed similar levels of GFP as DP thymocytes, whereas the other showed higher levels of GFP than CD4SP thymocytes (Fig. 5 C). Given that most

$CD122^-$ IELps expressed GFP to levels similar to conventionally selected single-positive (SP) thymocytes, it appears this IELp fraction is enriched in cells that have not received agonist signals. However, $CD122^+$ IELps showed a prominent population of cells with greater GFP expression than SP thymocytes, indicating that only the $CD122^+$ IELp pool contained cells that have recently received agonist signals.

Given that we observed two distinct populations of $CD122^+$ IELps in $Nur77^{GFP}$ mice based on expression GFP, we wanted to examine these fractions for other phenotypic differences, namely expression of $\alpha_4\beta_7$ and CD103. $CD122^+GFP^{hi}$ IELp cells had prominent populations of $\alpha_4\beta_7^-CD103^-$ cells and $\alpha_4\beta_7^+CD103^-$ cells with few $\alpha_4\beta_7^+CD103^+$ cells (Fig. 5 D). The $CD122^+GFP^{lo}$ IELp fraction also contained a prominent population of $\alpha_4\beta_7^-CD103^-$, but few $\alpha_4\beta_7^+CD103^-$ cells. Rather, many $CD122^+GFP^{lo}$ IELps were $\alpha_4\beta_7^-CD103^+$. Therefore, $CD122^+GFP^{lo}$ and $CD122^+GFP^{hi}$ IELps from $Nur77^{GFP}$ mice show unique expression patterns of $\alpha_4\beta_7$ and CD103 that may impact their ability to generate TCR$\alpha\beta^+$CD8$\alpha\alpha$ IELs. This heterogeneity was confirmed using PD-1 expression as an additional marker of high-affinity Ag signaling (Fig. 5 E).

CD122-, $\alpha_4\beta_7$-, and CD103-expressing subpopulations of IELps display distinct temporal patterns of development

To gain further insight into the development of the heterogeneous IELp pool, we made use of RAG2p-GFP reporter mice (Yu et al., 1999). Because developing thymocytes extinguish RAG expression at the DP stage, GFP expression in mature thymocytes identifies cells that were recently derived from DP. Furthermore, we can measure the time elapsed from precursor DP thymocytes to the progeny cell of interest based on decay of the GFP signal (~54-h half-life; McCaughtry et al., 2007). Similar to a previous study (McCaughtry et al., 2007), most CD4SP and CD8SP thymocytes were GFP^+, with CD8SP thymocytes expressing less GFP (mean fluorescence intensity [MFI]; Fig. 6 A). For agonist selected lineages, ~50% of Treg and 20% of iNKT cells were GFP^+, and nascent tTreg and iNKT were similar in age to CD4SP thymocytes (Fig. 6 A). Similar to tTreg, ~50% of $CD122^+$ IELps were GFP^+, again suggesting heterogeneity within this population (Fig. 6 A, top). Furthermore, nascent $CD122^+$ IELps displayed similar MFIs of GFP expression as CD8SP thymocytes, suggesting similar developmental kinetics (Fig. 6 A, middle and bottom). In contrast, $CD122^-$ IELps showed similar frequencies of GFP^+ cells and similar GFP MFIs as DP thymocytes. These data suggest that the $CD122^-$ IELp fraction is very recently derived from DP and appears to be immature relative to other post-selection populations.

Given the presence of two distinct $CD122^+$ IELps based on Rag2p-GFP expression, we next examined $\alpha_4\beta_7$ and CD103 expression in these subsets (Fig. 5, A and B). The majority of $\alpha_4\beta_7^+CD103^-$ and $\alpha_4\beta_7^+CD103^+$ cells were GFP^+, ~50% of $\alpha_4\beta_7^-CD103^-$ cells were GFP^+, and only ~10% of $\alpha_4\beta_7^-CD103^+$ cells were GFP^+ (Fig. 6 B, top). These results indicated that the majority of $\alpha_4\beta_7^+CD103^-$ and $\alpha_4\beta_7^+CD103^+$ $CD122^+$ IELps are recently derived from DP thymocytes, whereas only half of $\alpha_4\beta_7^-CD103^-$ cells are nascent and the majority of $\alpha_4\beta_7^-CD103^+$ cells are aged. Within the GFP^+ populations, we further analyzed GFP MFIs to determine temporal patterns of development. GFP^+ $\alpha_4\beta_7^-CD103^-$ cells were the youngest in the $CD122^+$ IELp pool, followed by $\alpha_4\beta_7^+CD103^-$ cells, $\alpha_4\beta_7^+CD103^+$ cells, and finally $\alpha_4\beta_7^-CD103^+$ cells (Fig. 6 B, middle and bottom). These results suggest that the $CD122^+$ IELp pool contains distinct subpopulations of cells with unique temporal patterns of development.

Using the RAG2p-GFP model, we defined distinct subpopulations of IELp cells with unique temporal signatures that may represent cells at various stages of maturity. Ultimately, for IELp cells to traffic to intestinal tissues, they must first exit the thymus. Before export, conventional thymocytes up-regulate the S1P receptor, S1P1, to promote thymocyte egress (Matloubian et al., 2004; Xing et al., 2016). Therefore, we measured the expression of S1P1 on the surface of IELp subsets by flow cytometry (Fig. 6 C). We observed significantly increased levels of S1P1 expression on $CD122^+$ IELp cells relative to $CD122^-$ IELps. Furthermore, $CD122^-$ IELps had a significantly lower MFI of S1P1 expression relative to DP thymocytes, which themselves do not exit the thymus under physiological conditions. We next examined S1P1 expression on $\alpha_4\beta_7$- and CD103-expressing subpopulations of $CD122^+$ IELps. We found that $\alpha_4\beta_7^+CD103^-$ and $\alpha_4\beta_7^+CD103^+$ cells both showed significantly higher S1P1 MFIs compared with either $\alpha_4\beta_7^-CD103^-$ or $\alpha_4\beta_7^-CD103^+$ counterparts. However, all of the $CD122^+$ IELp subpopulations examined showed substantially higher S1P1 expression than DP thymocytes or $CD122^-$ IELps, suggesting that all of these populations may have the potential to egress from the thymus.

$\alpha_4\beta_7$- and CD103-expressing subpopulations of IELps show distinct patterns of IEL development in vivo

Given that the IELp pool is heterogeneous in nature, we sought to determine whether different IELp subpopulations had differing abilities to generate TCR$\alpha\beta^+$CD8$\alpha\alpha$ IELs. Because the $CD122^+$ IELp population showed protection from apoptosis (Fig. 4 D), expressed proteins induced by high-affinity TCR signaling (Fig. 2, B and C; and Fig. 5, C–E), contained subsets that expressed the adhesion molecules $\alpha_4\beta_7$ and CD103 (Fig. 5 A), and expressed higher levels of egress receptor S1P1 than $CD122^-$ IELps (Fig. 6 C), we focused our analysis on prominent subpopulations within the $CD122^+$ IELp fraction. We chose to examine $CD122^+PD\text{-}1^+$ $\alpha_4\beta_7^+CD103^-$ IELps and $CD122^+PD\text{-}1^-\alpha_4\beta_7^-CD103^+$ IELps because they represented two of the major subsets of IELps, were mostly homogeneous from an "age" perspective, and were polar opposites with respect to age and cell surface phenotype. We sorted these IELp populations from $CD45.1^+$ or $CD45.1/2^+$ donors, mixed these populations at a 1:1 ratio, co-adoptively transferred them into $RAG1^{-/-}$ recipient mice ($CD45.2^+$), and examined

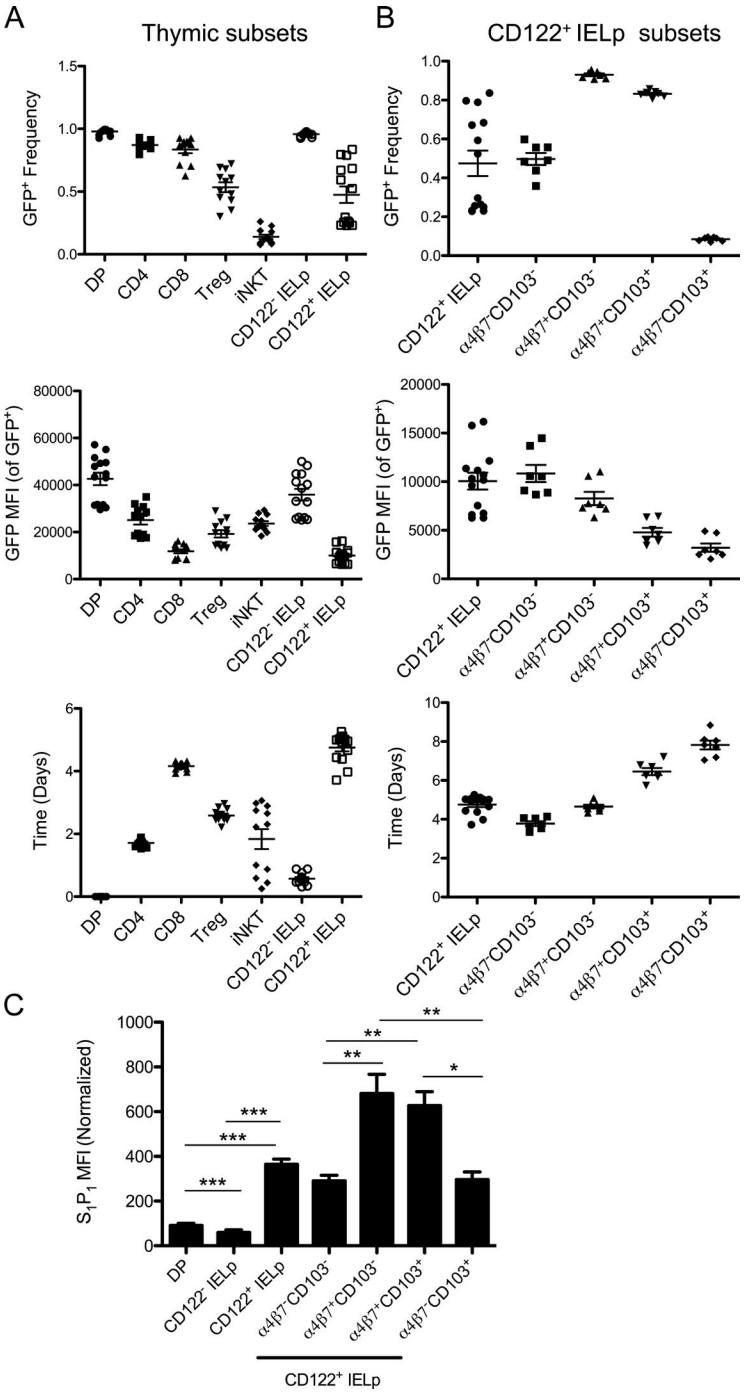

Figure 6. **$\alpha_4\beta_7$- and CD103–expressing subpopulations of IELps display distinct temporal patterns of development.** Numerous thymocyte populations from RAG2p-GFP mice were analyzed for frequencies of GFP$^+$ cells (top), and MFI of GFP expression within GFP$^+$ cells (middle), to study the temporal dynamics of development from DP progenitors. GFP MFI within GFP$^+$ cells were used to calculate the time elapsed from the DP stage to the time of interrogation using a GFP half-life of 54 h (bottom). (A) Analysis of conventionally selected lineages (CD4 and CD8) and agonist selected lineages (Treg, iNKT, and CD122$^{-/+}$ IELps). (B) Analysis of $\alpha_4\beta_7$- and CD103-expressing subpopulations of CD122$^+$ IELps. DP, CD4, CD8, Treg, iNKT, and IELp data were obtained over four individual experiments ($n = 14$). $\alpha_4\beta_7$ and CD103 subpopulation data were obtained over two individual experiments ($n = 7$). (C) Normalized MFIs of S1P1 expression on the indicated thymocyte populations. S1P1 expression was normalized using control cells lacking primary antibody staining (normalized MFI = S1P1 MFI − control MFI). For DP, CD122$^-$ IELps, and CD122$^+$ IELps, data are compiled from seven mice over four individual experiments. For $\alpha_4\beta_7$- and CD103-expressing subpopulations of CD122$^+$ IELps, data are compiled from five mice over two independent experiments. *, $P < 0.05$; **, $P < 0.01$; ***, $P < 0.001$ (paired Student's *t* test). Error bars indicate SEM.

the IEL compartment 6 wk after transfer. At the time of harvest, TCR$\alpha\beta^+$ IELs from both CD122$^+$PD-1$^+\alpha_4\beta_7^+$CD103$^-$ and CD122$^+$PD-1$^-\alpha_4\beta_7^-$CD103$^+$ IELp donors were clearly detectable in recipient mice (Fig. 7 A, left). However, the PD-1$^+\alpha_4\beta_7^+$CD103$^-$ subset showed almost complete skewing toward TCR$\alpha\beta^+$CD8$\alpha\alpha$ IEL development, whereas PD-1$^-\alpha_4\beta_7^-$CD103$^+$ cells showed nearly exclusive development of TCR$\alpha\beta^+$CD8$\alpha\beta$ IEL (Fig. 7 A, middle, right). Therefore, it appears that despite both residing within the CD122$^+$ IELp fraction, PD-1$^+\alpha_4\beta_7^+$CD103$^-$ and PD-1$^-\alpha_4\beta_7^-$CD103$^+$ cells showed distinct patterns of IEL development.

Because we found that CD122$^+$PD-1$^-\alpha_4\beta_7^-$CD103$^+$ IELp cells did not give rise to TCR$\alpha\beta^+$CD8$\alpha\alpha$ IELs, we tested the ability of another CD122$^+$ IELp subset to give rise to intestinal IEL populations in vivo. We chose PD-1$^+\alpha_4\beta_7^-$CD103$^-$ cells to compete against the PD-1$^+\alpha_4\beta_7^+$CD103$^-$ fraction because they constituted a relatively major fraction of IELp cells (Fig. 4) and were "younger" than $\alpha_4\beta_7^+$CD103$^-$ cells

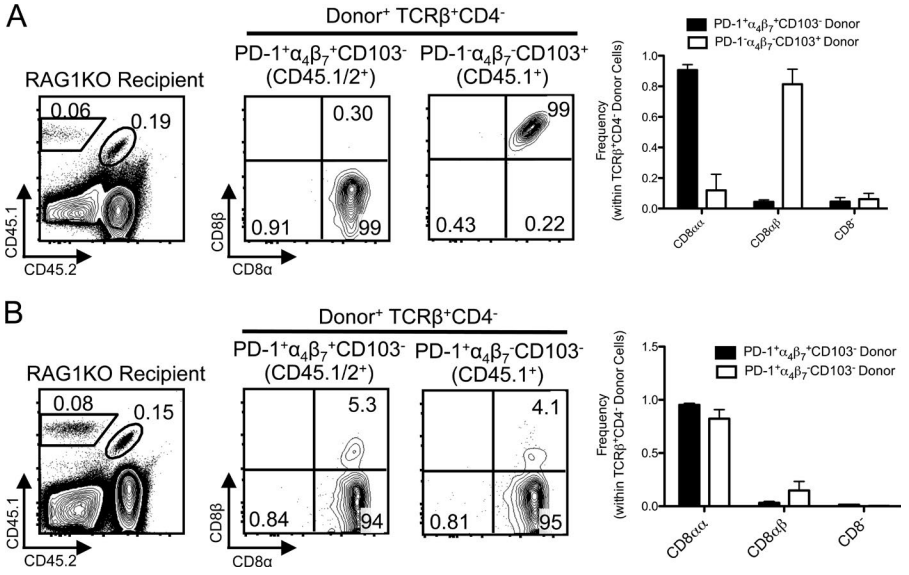

Figure 7. **Subpopulations of IELps generate TCRαβ+ CD8αα IELs with differential efficiency.** (A and B) Congenically marked PD-1+$\alpha_4\beta_7$+CD103− (CD45.1/2+) and PD-1−$\alpha_4\beta_7$−CD103+ (CD45.1+) CD122+ IELps (CD4−/dullCD8−/dullNK1.1−TCRβ+CD5+CD122+; A) or congenically marked PD-1+$\alpha_4\beta_7$+CD103− (CD45.1/2+) and PD-1+$\alpha_4\beta_7$−CD103− (CD45.1+) CD122+ IELps (B) were sorted and adoptively transferred into RAG1-deficient animals at a 1:1 ratio. Small intestines were harvested from recipient mice 6 wk later and analyzed for the presence of IEL populations. CD45.1 and CD45.2 expression profiles of total IEL cells from recipient mice (left). TCRβ+CD4− cells were gated on within each Donor+ population and were analyzed for expression of CD8β and CD8α (middle). Frequencies of CD8αα, CD8αβ, and CD8− cells within TCRβ+CD4− from the indicated donor derived populations (right). For A, data were collected from $n = 5$ recipient mice over four individual experiments. For B, data were collected from $n = 5$ recipient mice over three individual experiments. Error bars indicate SEM.

(Fig. 6 B). Both PD-1+$\alpha_4\beta_7$+CD103− and PD-1+$\alpha_4\beta_7$−CD103− donor cells predominantly gave rise to TCRαβ+CD8αα IELs (Fig. 7 B, middle, right), suggesting that TCRαβ+CD8αα IEL lineage potential is not limited to the CD122+PD-1+$\alpha_4\beta_7$+CD103− IELp fraction.

Human thymi contain IELp phenotype cells

Although TCRαβ+CD8αα IEL cells have been identified in human intestine (Latthe et al., 1994), it is unclear whether human thymi contain IELp cells. We examined human thymi for the presence of thymocytes with an "IELp" phenotype. Similar to IELps in mice, within the CD4−/dullCD8−/dull fraction, a robust population of TCRβ+CD5+ cells was found (Fig. 8, A and C). However, in contrast to mouse, human CD4−/dullCD8−/dullTCRβ+CD5+ thymocytes showed a near absence of CD122-expressing cells (Fig. 8, B and C). Despite showing a lack of CD122-expressing cells, human CD4−/dullCD8−/dullTCRβ+CD5+ thymocytes showed other attributes consistent with mouse IELps, including a small fraction of PD-1+Helios+ cells (Fig. 8, B and C). Furthermore, within the CD4−/dullCD8−/dullTCRβ+CD5+ population, we observed a near absence of CD103-expressing cells (Fig. 8, B and C), but a prominent population of β_7+CD103− cells. These cells resemble the mouse $\alpha_4\beta_7$+CD103− IELp population that gave rise to TCRαβ+CD8αα IELs.

DISCUSSION

We have identified RasGRP1 as a critical regulator of natural TCRαβ+CD8αα IEL development through its control of agonist selection and IELp generation in the thymus. Given that RasGRP1 is required for conventional thymocyte positive selection in response to low-affinity TCR signaling and is also required for iNKT (Shen et al., 2011) and TCRαβ+CD8αα IEL development in response to high-affinity TCR stimuli, there is clearly an overlap between the signal transduction molecules that regulate positive selection and agonist selection. These data suggest a global requirement for RasGRP1 signaling in generating a diverse T cell repertoire stemming from either weak or strong TCR selection signals in the thymus. Whether the genetic programs induced by RasGRP1 that are required for positive selection and agonist selection are similar or not will require further investigation.

In contrast to agonist selection, RasGRP1 activity is not required for thymocyte clonal deletion. The finding that Bim deficiency rescues IELp development in RasGRP1−/− mice suggests that RasGRP1 signaling is pro-survival rather than fate specifying in this context. As such, these data provide a possible explanation for the differential requirement of RasGRP1 in clonal deletion versus IELp generation, both of which require strong TCR signals. For clonal deletion, an active apoptotic program is initiated, and therefore pro-survival signaling mediated by RasGRP1 would be detrimental to this outcome. In contrast, IELp generation requires survival of the cells that receive a strong TCR signal, and under these conditions, RasGRP1 appears to be required to deliver these signals. However, it should be noted that RasGRP1−/− Bim−/− mice show reduced numbers of IELps compared with Bim−/− mice, suggesting a role for RasGRP1 signaling outside of survival.

The primary function of RasGRP1 is to activate the highly conserved signal transduction protein Ras. The activation kinetics of the Ras–ERK cascade are differentially regulated during thymocyte positive and negative selection.

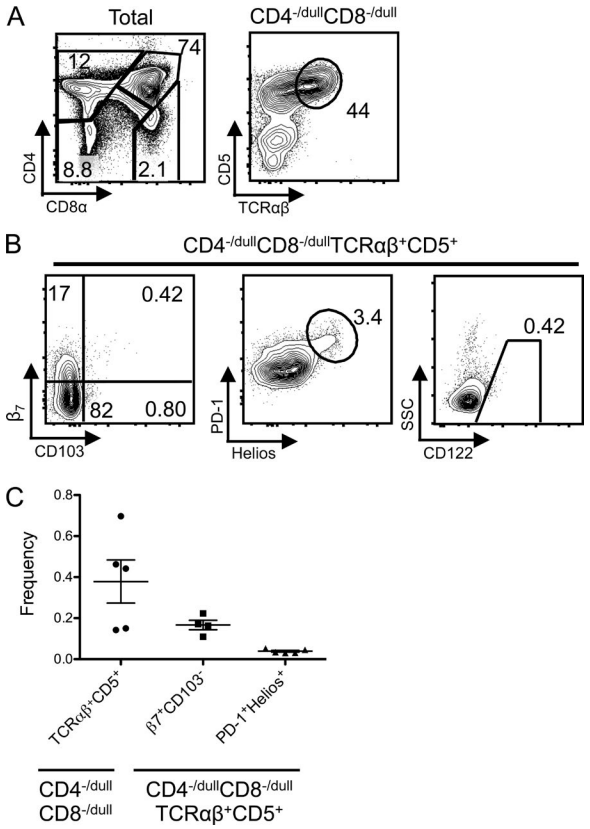

Figure 8. **Human thymi contain IELp phenotype cells.** Human thymi were analyzed for the presence of cells expressing markers that were previously characterized in the murine IELp population. (A and C) Total thymocytes were analyzed for the expression of CD4 and CD8 (left). $CD4^{-/dull}$ $CD8^{-/dull}$ thymocytes were analyzed for expression of CD5 and TCRαβ (right). (B and C) $CD4^{-/dull}CD8^{-/dull}TCR\alpha\beta^{+}CD5^{+}$ thymocytes were gated and examined for expression of the indicated markers. Most data were collected from $n = 5$ patients over five individual experiments. CD103 and β_7 staining was collected from $n = 4$ patients over four individual experiments. Error bars indicate SEM.

During positive selection, thymocytes show a sustained increase in ERK activation whereas thymocytes undergoing negative selection show a strong, but transient, burst of ERK activation (Mariathasan et al., 2001; McNeil et al., 2005; Daniels et al., 2006). Importantly, numerous studies have shown that ERK activity is dispensable during thymocyte negative selection but is required for efficient thymocyte positive selection (Werlen et al., 2000; McNeil et al., 2005; McGargill et al., 2009). Given the requirement for RasGRP1 in agonist selection of both iNKT (Shen et al., 2011) and IELps, ERK activity is likely important for thymocyte agonist selection generally.

Consistent with the above-described pattern of Erk activation, thymocytes undergoing positive selection show numerous, brief serial interactions with stromal cells over the course of days, whereas thymocytes undergoing negative selection show relatively stable interactions with stromal cells over the course of hours (Melichar et al., 2013). Because the strength of signal that drives clonal deletion and agonist selection are similar, one might predict that those cells undergoing agonist selection also engage in stable interactions with APC. However, given that IELps have a relative age similar to CD8SP, there must be mechanisms in place to regulate the outcome of the interactions with APC, that being differentiation or death. One such regulatory mechanism could be the CD28-B7 signaling pathway (Pobezinsky et al., 2012). Alternatively, or in addition to, it is possible that it is the nature of the APC that regulates the outcome of these interactions. For example, in the HY^{cd4} model, thymocytes undergoing apoptosis are positioned closely to DCs in the thymus, and restricting male Ag expression to cTEC or radio-resistant APC impaired apoptosis induction (McCaughtry et al., 2008). Given that agonist-selected cells do not undergo apoptosis during development, it is likely that thymocyte agonist selection does not involve stable interactions with apoptosis-inducing DCs, but rather involves interactions with cTEC cells that are less potent inducers of clonal deletion. Whether the nature of the APC presenting high-affinity Ag regulates IELp development requires investigation.

Distinct $CD122^{-}$ and $CD122^{+}$ populations make up the "IELp" fraction and highlight the diversity of cells present within this pool. In polyclonal mice, RasGRP1 did not appear to regulate the fraction of IELps that expressed CD122, whereas in the HY^{cd4} model, RasGRP1-deficient males displayed reduced frequencies of $CD122^{+}$ IELps. The reason for this difference is currently unclear. $CD122^{-}$ IELps lacked expression of proteins induced by strong TCR signaling and showed high frequencies of cell death, whereas $CD122^{+}$ IELps were enriched in cells expressing markers of high-affinity antigen encounter and were largely protected from apoptosis. Furthermore, using RAG2p-GFP animals, we found that $CD122^{-}$ IELps were similar in age to immature DP cells, whereas $CD122^{+}$ IELps showed a similar age as post-selection CD8SP thymocytes. In addition, $CD122^{-}$ IELps lacked expression of egress receptor S1P1, whereas $CD122^{+}$ IELps showed robust expression of S1P1, consistent with the known phenotype of mature post-selection cells (Xing et al., 2016). Of note, McDonald et al. (2014) recently determined that in TCR transgenic mice that express a TCR cloned from TCRαβ CD8αα IELs, almost all recent thymic emigrants expressed CD122 and most were $\alpha_4\beta_7^{+}$. Collectively, these data suggest that CD122 expression marks an important transition in the development and maturation of IELps. Of note, CD122 expression per se may not be important for IELp thymic development as IL-15–deficient thymi mice contain similar numbers of IELps (Klose et al., 2014) and are able to reconstitute the IEL compartment of nude mice (Lai et al., 2008).

Although CD122 expression appears to separate distinct IELp fractions, expression of $\alpha_4\beta_7$ and CD103 revealed an additional layer of diversity within the IELps. Notably, $CD122^{-}$ IELp cells lacked $\alpha_4\beta_7$- and CD103-expressing

cells altogether, whereas CD122$^+$ IELps showed four distinct populations of $\alpha_4\beta_7$- and CD103-expressing progenitors. Although RasGRP1-deficient IELps largely lacked expression of $\alpha_4\beta_7$ and CD103, it is unclear whether this is caused by RasGRP1-dependent signal transduction or increased apoptosis of the progenitor. Using PD-1 and Nur77-GFP as readouts of TCR signaling, we found that $\alpha_4\beta_7$ expression was associated with CD122$^+$ cells showing recent high-affinity TCR signaling, whereas CD103 expression was enriched on cells lacking signs of recent TCR signaling (Fig. 5, D and E). Additionally, analysis of Rag2p-GFP animals revealed that nascent $\alpha_4\beta_7{}^-$CD103$^-$ were the youngest of the CD122$^+$ IELp pool, whereas $\alpha_4\beta_7{}^+$CD103$^-$ and $\alpha_4\beta_7{}^+$CD103$^+$ were slightly older and $\alpha_4\beta_7{}^-$CD103$^+$ cells were especially aged. Testing the significance of $\alpha_4\beta_7$ and CD103 expression in vivo revealed that both PD-1$^+\alpha_4\beta_7{}^+$CD103$^-$ and PD-1$^+\alpha_4\beta_7{}^-$CD103$^-$ developed into TCR$\alpha\beta^+$CD8$\alpha\alpha$ IELs almost exclusively. However, PD-1$^-\alpha_4\beta_7{}^-$CD103$^+$ gave rise to TCR$\alpha\beta^+$CD8$\alpha\beta$ IELs. These data suggest that PD-1 expression correlates well with the ability to differentiate into TCR$\alpha\beta^+$CD8$\alpha\alpha$ IELs. Importantly, however, S1P1 expression analysis showed that $\alpha_4\beta_7{}^+$CD103$^-$ cells expressed significantly higher levels of S1P1 than $\alpha_4\beta_7{}^-$CD103$^-$ cells, making it tempting to speculate that the CD122$^+$PD-1$^+\alpha_4\beta_7{}^+$CD103$^-$ IELp subset is the population that emigrates out of the thymus under physiological conditions. Data from McDonald et al. (2014) support this finding.

Recently, a study from Ruscher et al. (2017) also examined the thymic IELp compartment using a T-bet reporter mouse. The findings of our study reported here and the Ruscher study are largely congruent. Using the T-bet reporter to subset thymic IELps, Ruscher et al. (2017) identified a T-bet$^-$ population, so called "type A" cells, and a T-bet$^+$ population denoted "type B" cells. The type A cells are phenotypically similar to the CD122$^+$ PD-1$^+$ $\alpha_4\beta_7{}^+$ CD103$^-$ IELps described here, whereas the type B cells are similar to the CD122$^+$ PD-1$^-$ $\alpha_4\beta_7{}^-$ CD103$^+$ IELps. This included characteristics such as age after DP stage, signs of recent strong TCR signaling, and expression of the thymic egress receptor, S1P1. Furthermore, upon adoptive transfer of either CD122$^+$ PD-1$^+$ $\alpha_4\beta_7{}^+$ CD103$^-$ IELps or CD122$^+$ PD-1$^+$ type A IELps into Rag$^{-/-}$ recipients, TCR$\alpha\beta^+$CD8$\alpha\alpha$ IELs were generated. However, there was one obvious difference reported in Ruscher et al. (2017) when compared with the data described here. We found that sorted CD122$^+$ PD-1$^-$ $\alpha_4\beta_7{}^-$ CD103$^+$ IELps adoptively transferred to Rag$^{-/-}$ recipients gave rise to TCR$\alpha\beta^+$CD8$\alpha\beta$ IELs, whereas purified CD122$^+$ PD-1$^-$ (type B) IELps generated TCR$\alpha\beta^+$CD8$\alpha\alpha$ IELs. We think it is likely that different sorting strategies resulted in different outcomes for these seemingly similar populations of IELps. In particular, our sorting strategy involved isolating NK1.1$^-$ IELps, whereas Ruscher et al. (2017) used CD1d-tetramer to specifically exclude iNKT cells. Furthermore, we positively sorted on CD103-expressing IELps, whereas Ruscher et al. (2017) did not discriminate between CD103$^+$ or CD103$^-$ fractions, both of which are present in the type B IELps. Therefore, it appears that the composition of the adoptively transferred cells was substantially different in the two studies and resulted in the disparate findings. Finally, the other major difference was Ruscher et al. (2017) used a mixture of DN thymocyte competitors, whereas we directly competed different IELp populations in the adoptive transfer.

Previous work has identified the presence of CD8$\alpha\alpha$-expressing $\alpha\beta$ T cells within the human intestine (Latthe et al., 1994). However, whether these cells resemble TCR$\alpha\beta^+$CD8$\alpha\alpha$ IELs in either their development or functionality remains unclear. We found a human thymocyte population that resembled murine IELp cells. This included coexpression of PD-1 and Helios and expression of β_7 without CD103. Human IELps lacked CD103$^+$ cells, which made up a significant portion of the mouse IELp compartment. Furthermore, human IELps did not appear to express CD122. Although the developmental origin of TCR$\alpha\beta^+$CD8$\alpha\alpha$ IELs in humans has not been strictly examined, these results suggest that human thymi contain cells that largely recapitulate the phenotype of murine IELps. In fact, it was recently reported that human thymus contains a distinct population of PD-1$^+$ thymocytes that appear to undergo agonist selection (Verstichel et al., 2017). Further studies are required to determine whether human TCR$\alpha\beta^+$CD8$\alpha\alpha$ IELs originate from a thymic progenitor similar to mice.

The functional heterogeneity of the IELp population is defined by the TCR signaling events experienced by developing thymocytes. RasGRP1-mediated signals are clearly required for efficient generation of IELps, and RasGRP1-deficient IELps show signs of impaired high-affinity TCR signaling. Furthermore, the expression of markers of TCR signaling strength by IELp cells was associated with their thymic expression of CD122 and of adhesion molecules $\alpha_4\beta_7$ and CD103. IELp cells showing signs of recent high-affinity TCR signaling are skewed toward expression of $\alpha_4\beta_7$ and were high fidelity progenitors of TCR$\alpha\beta^+$CD8$\alpha\alpha$ IELs. The requirement of RasGRP1 activity during agonist selection separates the signaling requirements during agonist selection and clonal deletion. These results provide critical insight into the signaling events that drive TCR$\alpha\beta^+$CD8$\alpha\alpha$ IEL development, but the precise outcome of RasGRP1-mediated signals in agonist-selected thymocytes that specify the development of IELps is unclear. One possibility is the induction of a lineage-specifying transcription factors. Future work examining the transcriptional landscape of the specific IELp that gives rise to TCR$\alpha\beta^+$ CD8$\alpha\alpha$ IELs will be required.

MATERIALS AND METHODS

Mice

The generation of RasGRP1 KO (Dower et al., 2000), Bim KO (Bouillet et al., 1999), HY^{cd4} (Baldwin et al., 2005), Nur77^{GFP} (Moran et al., 2011), RAG2p-GFP (Yu et al.,

1999), and RAG1$^{-/-}$ (Mombaerts et al., 1992) mice has been previously described. WT CD45.1^{+} and CD45.1/2^{+} mice were maintained in our colony. RAG2p-GFP and RAG1$^{-/-}$ mice were provided by C. Anderson (University of Alberta, Edmonton, AB, Canada). All mice were maintained on the C57BL/6 background. For all strains, mice of both sexes were used between 4 wk and 6 mo of age. All mice were treated in accordance with protocols approved by the University of Alberta Animal Care and Use Committee.

Antibodies and flow cytometry

Fluorochrome-conjugated and biotinylated Ab were purchased from eBioscience, BioLegend, or BD PharMingen. Active caspase 3 Ab was purchased from Cell Signaling Technologies. Cells were stained with Ab cocktails in FACS buffer (PBS, 1% FCS, 0.02% sodium azide) for 30 min on ice. Cells were washed twice with FACS buffer after primary and secondary Ab staining. For intracellular Ag staining, cells were treated with BD Cytofix/Cytoperm (BD Bioscience) or the Foxp3 Staining Buffer Set (eBioscience). S1P1 antibody was purchased from R&D Systems, and surface staining was performed as previously described (Arnon et al., 2011; Green and Cyster, 2012). Cell events were collected on LSRFortessa or LSR II (BD PharMingen) analyzers, and data were analyzed with FlowJo software (Tree Star).

IEL preparations

Small intestines were removed from mice and cleaned, and Peyer's patches were excised. Intestines were opened longitudinally, rinsed of contents, and cut into ∼0.5-cm pieces. Intestinal pieces were placed in Ca^{2+}/Mg^{2+}-free HBSS supplemented with 5% FCS, 5 mM EDTA, and 2 mM DTT and shaken at 37°C for 30 min. After incubation, cell-containing media was passed through 70-µm cell strainers, and cells were pelleted. Cell pellets were resuspended in 40% Percoll, layered on top of an 80% Percoll solution, and the gradient was centrifuged at 900 *g* for 20 min. IELs were extracted from the 40%/80% interface, washed in PBS, and used for analysis. Flow cytometry and CountBright beads (Life Technologies) were used for quantification.

Adoptive transfer experiments

Thymocytes were obtained from congenic CD45.1^{+} and CD45.1/2^{+} donor mice and stained as described in Antibodies and flow cytometry in PBS supplemented with 2% FCS. Three IELp populations were sorted from donor mice: CD4$^{-/dull}$CD8$^{-/dull}$NK1.1^{-}TCRβ^{+}CD5^{+}CD122^{+}PD-1^{+}α$_4$β$_7$$^{+}$CD103^{-}, CD4$^{-/dull}$CD8$^{-/dull}$NK1.1^{-}TCRβ^{+}CD5^{+}CD122^{+}PD-1^{+}α$_4$β$_7$$^{-}$CD103^{-}, and CD4$^{-/dull}$CD8$^{-/dull}$NK1.1^{-}TCRβ^{+}CD5^{+}CD122^{+}PD-1^{-}α$_4$β$_7$$^{-}$CD103^{+}. Congenically marked, sorted IELps were mixed 1:1 (1.5–5.0 × 10^4 cells of each donor population per recipient) and injected i.v. into RAG1$^{-/-}$ mice (CD45.2^{+}). Recipient mice were analyzed for the presence of IEL populations 6 wk later. Cell sorting was performed using a FACSAria III (BD Biosciences) instrument.

Human thymi

Human thymi were collected from patients (age 10.8 mo ± 17.5 mo, range 0.2–42 mo) during pediatric surgery at British Columbia Children's Hospital, Vancouver. Thymic tissue was manually dissociated in RPMI complete media (RPMI 1640; Gibco) containing 1% GlutaMAX (Invitrogen), 1% penicillin/streptomycin (Invitrogen), and 10% heat-inactivated fetal bovine serum (Gibco). After filtering and washing, cells were stained for flow cytometry. Collection of human tissue was approved by the University of British Columbia Clinical Research Ethics Board (Vancouver, Canada). Informed consent was obtained in accordance with local regulatory guidelines.

Statistics

Mean, SEM, and p-values were calculated using Prism software (GraphPad), using two-tailed, unpaired, or paired Student's *t* tests. Asterisks represent statistically significant differences comparing the indicated groups represented as *, $P < 0.05$; **, $P < 0.01$; and ***, $P < 0.001$.

Online supplemental material

Fig. S1 is a compilation of the frequency of CD122^{+} IELps in the indicated mice. Fig. S2 shows that Bim deletion rescues the generation TCRαβ^{+} CD8αα IELs in RasGRP1-deficient mice.

ACKNOWLEDGMENTS

The authors thank the Faculty of Medicine and Dentistry flow cytometry core and Health Sciences Lab Animal Services at the University of Alberta for support, Mr. Bing Zhang for technical assistance, Drs. Qian Nancy Hu and Sylvie Lesage for critical review of the manuscript and Drs. Roland Ruscher and Kristin Hogquist for feedback and discussions. We are grateful to Dr. Colin Anderson for providing RAG2p-GFP and RAG1$^{-/-}$ mice for our experiments. In addition, we would like to thank Dr. Andrew Campbell and the surgical staff at the University of British Columbia Children's Hospital for collection of pediatric thymi.

This work was supported by the Natural Sciences and Engineering Research Council of Canada (418161 to T.A. Baldwin), the Canadian Institutes of Health Research (CIHR; MOP 86595 to T.A. Baldwin), and the Canadian National Transplant Research Program (TFU 127880 to M.K. Levings). D.P. Golec holds an Alberta Innovates Health Solutions studentship. M.K. Levings and R.E. Hoeppli receive salary awards from the Child and Family Research Institute. R.E. Hoeppli was supported by a graduate studentship from the CIHR Transplant Research Training Program.

The authors declare no competing financial interests.

Author contributions: D.P. Golec, R.E. Hoeppli, M.K. Levings, and T.A. Baldwin designed the experiments. D.P. Golec, R.E. Hoeppli, L.M. Henao Caviedes, and J. McCann performed the experiments. D.P. Golec and T.A. Baldwin analyzed the data and wrote the manuscript.

Submitted: 12 May 2017
Revised: 16 June 2017
Accepted: 20 June 2017

REFERENCES

Andrew, D.P., L.S. Rott, P.J. Kilshaw, and E.C. Butcher. 1996. Distribution of $\alpha_4\beta_7$ and $\alpha_E\beta_7$ integrins on thymocytes, intestinal epithelial lymphocytes and peripheral lymphocytes. *Eur. J. Immunol.* 26:897–905. http://dx.doi.org/10.1002/eji.1830260427

Arnon, T.I., Y. Xu, C. Lo, T. Pham, J. An, S. Coughlin, G.W. Dorn, and J.G. Cyster. 2011. GRK2-dependent S1PR1 desensitization is required for lymphocytes to overcome their attraction to blood. *Science.* 333:1898–1903. http://dx.doi.org/10.1126/science.1208248

Bäckström, B.T., U. Müller, B. Hausmann, and E. Palmer. 1998. Positive selection through a motif in the alphabeta T cell receptor. *Science.* 281:835–838. http://dx.doi.org/10.1126/science.281.5378.835

Baldwin, T.A., and K.A. Hogquist. 2007. Transcriptional analysis of clonal deletion in vivo. *J. Immunol.* 179:837–844. http://dx.doi.org/10.4049/jimmunol.179.2.837

Baldwin, T.A., M.M. Sandau, S.C. Jameson, and K.A. Hogquist. 2005. The timing of TCRα expression critically influences T cell development and selection. *J. Exp. Med.* 202:111–121. http://dx.doi.org/10.1084/jem.20050359

Bouillet, P., D. Metcalf, D.C. Huang, D.M. Tarlinton, T.W. Kay, F. Köntgen, J.M. Adams, and A. Strasser. 1999. Proapoptotic Bcl-2 relative Bim required for certain apoptotic responses, leukocyte homeostasis, and to preclude autoimmunity. *Science.* 286:1735–1738. http://dx.doi.org/10.1126/science.286.5445.1735

Cheroutre, H., F. Lambolez, and D. Mucida. 2011. The light and dark sides of intestinal intraepithelial lymphocytes. *Nat. Rev. Immunol.* 11:445–456. http://dx.doi.org/10.1038/nri3007

Daley, S.R., D.Y. Hu, and C.C. Goodnow. 2013. Helios marks strongly autoreactive CD4+ T cells in two major waves of thymic deletion distinguished by induction of PD-1 or NF-κB. *J. Exp. Med.* 210:269–285. http://dx.doi.org/10.1084/jem.20121458

Daniels, M.A., E. Teixeiro, J. Gill, B. Hausmann, D. Roubaty, K. Holmberg, G. Werlen, G.A. Holländer, N.R. Gascoigne, and E. Palmer. 2006. Thymic selection threshold defined by compartmentalization of Ras/MAPK signalling. *Nature.* 444:724–729. http://dx.doi.org/10.1038/nature05269

Dower, N.A., S.L. Stang, D.A. Bottorff, J.O. Ebinu, P. Dickie, H.L. Ostergaard, and J.C. Stone. 2000. RasGRP is essential for mouse thymocyte differentiation and TCR signaling. *Nat. Immunol.* 1:317–321. http://dx.doi.org/10.1038/80799

Eberl, G., and D.R. Littman. 2004. Thymic origin of intestinal alphabeta T cells revealed by fate mapping of RORgammat+ cells. *Science.* 305:248–251. http://dx.doi.org/10.1126/science.1096472

Fu, G., J. Casas, S. Rigaud, V. Rybakin, F. Lambolez, J. Brzostek, J.A. Hoerter, W. Paster, O. Acuto, H. Cheroutre, et al. 2013. Themis sets the signal threshold for positive and negative selection in T-cell development. *Nature.* 504:441–445. http://dx.doi.org/10.1038/nature12718

Gangadharan, D., F. Lambolez, A. Attinger, Y. Wang-Zhu, B.A. Sullivan, and H. Cheroutre. 2006. Identification of pre- and postselection TCRalphabeta+ intraepithelial lymphocyte precursors in the thymus. *Immunity.* 25:631–641. http://dx.doi.org/10.1016/j.immuni.2006.08.018

Golec, D.P., N.A. Dower, J.C. Stone, and T.A. Baldwin. 2013. RasGRP1, but not RasGRP3, is required for efficient thymic β-selection and ERK activation downstream of CXCR4. *PLoS One.* 8:e53300. http://dx.doi.org/10.1371/journal.pone.0053300

Green, J.A., and J.G. Cyster. 2012. S1PR2 links germinal center confinement and growth regulation. *Immunol. Rev.* 247:36–51. http://dx.doi.org/10.1111/j.1600-065X.2012.01114.x

Guo, X., Y. Tanaka, and M. Kondo. 2015. Thymic precursors of TCRαβ$^+$CD8αα$^+$ intraepithelial lymphocytes are negative for CD103. *Immunol. Lett.* 163:40–48. http://dx.doi.org/10.1016/j.imlet.2014.11.007

Hanke, T., R. Mitnacht, R. Boyd, and T. Hünig. 1994. Induction of interleukin 2 receptor beta chain expression by self-recognition in the thymus. *J. Exp. Med.* 180:1629–1636. http://dx.doi.org/10.1084/jem.180.5.1629

Hu, Q.N., and T.A. Baldwin. 2015. Differential roles for Bim and Nur77 in thymocyte clonal deletion induced by ubiquitous self-antigen. *J. Immunol.* 194:2643–2653. http://dx.doi.org/10.4049/jimmunol.1400030

Klein, L., B. Kyewski, P.M. Allen, and K.A. Hogquist. 2014. Positive and negative selection of the T cell repertoire: what thymocytes see (and don't see). *Nat. Rev. Immunol.* 14:377–391. http://dx.doi.org/10.1038/nri3667

Klose, C.S., K. Blatz, Y. d'Hargues, P.P. Hernandez, M. Kofoed-Nielsen, J.F. Ripka, K. Ebert, S.J. Arnold, A. Diefenbach, E. Palmer, and Y. Tanriver. 2014. The transcription factor T-bet is induced by IL-15 and thymic agonist selection and controls CD8αα$^+$ intraepithelial lymphocyte development. *Immunity.* 41:230–243. http://dx.doi.org/10.1016/j.immuni.2014.06.018

Konkel, J.E., T. Maruyama, A.C. Carpenter, Y. Xiong, B.F. Zamarron, B.E. Hall, A.B. Kulkarni, P. Zhang, R. Bosselut, and W. Chen. 2011. Control of the development of CD8αα+ intestinal intraepithelial lymphocytes by TGF-β. *Nat. Immunol.* 12:312–319. http://dx.doi.org/10.1038/ni.1997

Kortum, R.L., C.L. Sommers, J.M. Pinski, C.P. Alexander, R.K. Merrill, W. Li, P.E. Love, and L.E. Samelson. 2012. Deconstructing Ras signaling in the thymus. *Mol. Cell. Biol.* 32:2748–2759. http://dx.doi.org/10.1128/MCB.00317-12

Lai, Y.G., M.S. Hou, Y.W. Hsu, C.L. Chang, Y.H. Liou, M.H. Tsai, F. Lee, and N.S. Liao. 2008. IL-15 does not affect IEL development in the thymus but regulates homeostasis of putative precursors and mature CD8 alpha alpha+ IELs in the intestine. *J. Immunol.* 180:3757–3765. http://dx.doi.org/10.4049/jimmunol.180.6.3757

Latthe, M., L. Terry, and T.T. MacDonald. 1994. High frequency of CD8 alpha alpha homodimer-bearing T cells in human fetal intestine. *Eur. J. Immunol.* 24:1703–1705. http://dx.doi.org/10.1002/eji.1830240737

Leishman, A.J., L. Gapin, M. Capone, E. Palmer, H.R. MacDonald, M. Kronenberg, and H. Cheroutre. 2002. Precursors of functional MHC class I- or class II-restricted CD8αα$^+$ T cells are positively selected in the thymus by agonist self-peptides. *Immunity.* 16:355–364. http://dx.doi.org/10.1016/S1074-7613(02)00284-4

Lesourne, R., E. Zvezdova, K.D. Song, D. El-Khoury, S. Uehara, V.A. Barr, L.E. Samelson, and P.E. Love. 2012. Interchangeability of Themis1 and Themis2 in thymocyte development reveals two related proteins with conserved molecular function. *J. Immunol.* 189:1154–1161. http://dx.doi.org/10.4049/jimmunol.1200123

Ma, L.J., L.F. Acero, T. Zal, and K.S. Schluns. 2009. Trans-presentation of IL-15 by intestinal epithelial cells drives development of CD8alphaalpha IELs. *J. Immunol.* 183:1044–1054. http://dx.doi.org/10.4049/jimmunol.0900420

Mariathasan, S., A. Zakarian, D. Bouchard, A.M. Michie, J.C. Zúñiga-Pflücker, and P.S. Ohashi. 2001. Duration and strength of extracellular signal-regulated kinase signals are altered during positive versus negative thymocyte selection. *J. Immunol.* 167:4966–4973. http://dx.doi.org/10.4049/jimmunol.167.9.4966

Matloubian, M., C.G. Lo, G. Cinamon, M.J. Lesneski, Y. Xu, V. Brinkmann, M.L. Allende, R.L. Proia, and J.G. Cyster. 2004. Lymphocyte egress from thymus and peripheral lymphoid organs is dependent on S1P receptor 1. *Nature.* 427:355–360. http://dx.doi.org/10.1038/nature02284

McCaughtry, T.M., M.S. Wilken, and K.A. Hogquist. 2007. Thymic emigration revisited. *J. Exp. Med.* 204:2513–2520. http://dx.doi.org/10.1084/jem.20070601

McCaughtry, T.M., T.A. Baldwin, M.S. Wilken, and K.A. Hogquist. 2008. Clonal deletion of thymocytes can occur in the cortex with no involvement of the medulla. *J. Exp. Med.* 205:2575–2584. http://dx.doi.org/10.1084/jem.20080866

McDonald, B.D., J.J. Bunker, I.E. Ishizuka, B. Jabri, and A. Bendelac. 2014. Elevated T cell receptor signaling identifies a thymic precursor to the TCRαβ$^+$CD4$^-$CD8β$^-$ intraepithelial lymphocyte lineage. *Immunity.* 41:219–229. http://dx.doi.org/10.1016/j.immuni.2014.07.008

McGargill, M.A., I.L. Ch'en, C.D. Katayama, G. Pagès, J. Pouysségur, and S.M. Hedrick. 2009. Cutting edge: Extracellular signal-related kinase is not required for negative selection of developing T cells. *J. Immunol.* 183:4838–4842. http://dx.doi.org/10.4049/jimmunol.0902208

McNeil, L.K., T.K. Starr, and K.A. Hogquist. 2005. A requirement for sustained ERK signaling during thymocyte positive selection in vivo. *Proc. Natl. Acad. Sci. USA.* 102:13574–13579. http://dx.doi.org/10.1073/pnas.0505110102

Melichar, H.J., J.O. Ross, P. Herzmark, K.A. Hogquist, and E.A. Robey. 2013. Distinct temporal patterns of T cell receptor signaling during positive versus negative selection in situ. *Sci. Signal.* 6:ra92. http://dx.doi.org/10.1126/scisignal.2004400

Mombaerts, P., J. Iacomini, R.S. Johnson, K. Herrup, S. Tonegawa, and V.E. Papaioannou. 1992. RAG-1-deficient mice have no mature B and T lymphocytes. *Cell.* 68:869–877. http://dx.doi.org/10.1016/0092-8674(92)90030-G

Mora, J.R., M.R. Bono, N. Manjunath, W. Weninger, L.L. Cavanagh, M. Rosemblatt, and U.H. Von Andrian. 2003. Selective imprinting of gut-homing T cells by Peyer's patch dendritic cells. *Nature.* 424:88–93. http://dx.doi.org/10.1038/nature01726

Moran, A.E., K.L. Holzapfel, Y. Xing, N.R. Cunningham, J.S. Maltzman, J. Punt, and K.A. Hogquist. 2011. T cell receptor signal strength in Treg and iNKT cell development demonstrated by a novel fluorescent reporter mouse. *J. Exp. Med.* 208:1279–1289. http://dx.doi.org/10.1084/jem.20110308

Ouyang, W., O. Beckett, Q. Ma, and M.O. Li. 2010. Transforming growth factor-beta signaling curbs thymic negative selection promoting regulatory T cell development. *Immunity.* 32:642–653. http://dx.doi.org/10.1016/j.immuni.2010.04.012

Pobezinsky, L.A., G.S. Angelov, X. Tai, S. Jeurling, F. Van Laethem, L. Feigenbaum, J.H. Park, and A. Singer. 2012. Clonal deletion and the fate of autoreactive thymocytes that survive negative selection. *Nat. Immunol.* 13:569–578. http://dx.doi.org/10.1038/ni.2292

Poussier, P., P. Edouard, C. Lee, M. Binnie, and M. Julius. 1992. Thymus-independent development and negative selection of T cells expressing T cell receptor alpha/beta in the intestinal epithelium: evidence for distinct circulation patterns of gut- and thymus-derived T lymphocytes. *J. Exp. Med.* 176:187–199. http://dx.doi.org/10.1084/jem.176.1.187

Priatel, J.J., S.J. Teh, N.A. Dower, J.C. Stone, and H.S. Teh. 2002. RasGRP1 transduces low-grade TCR signals which are critical for T cell development, homeostasis, and differentiation. *Immunity.* 17:617–627. http://dx.doi.org/10.1016/S1074-7613(02)00451-X

Reis, B.S., D.P. Hoytema van Konijnenburg, S.I. Grivennikov, and D. Mucida. 2014. Transcription factor T-bet regulates intraepithelial lymphocyte functional maturation. *Immunity.* 41:244–256. http://dx.doi.org/10.1016/j.immuni.2014.06.017

Rocha, B., P. Vassalli, and D. Guy-Grand. 1991. The V beta repertoire of mouse gut homodimeric alpha CD8+ intraepithelial T cell receptor alpha/beta + lymphocytes reveals a major extrathymic pathway of T cell differentiation. *J. Exp. Med.* 173:483–486. http://dx.doi.org/10.1084/jem.173.2.483

Ruscher, R., R.L. Kummer, Y.J. Lee, S.C. Jameson, and K.A. Hogquist. 2017. CD8αα intraepithelial lymphocytes arise from two main thymic precursors. *Nat. Immunol.* 18:771–779. http://dx.doi.org/10.1038/ni.3751

Shen, S., Y. Chen, B.K. Gorentla, J. Lu, J.C. Stone, and X.P. Zhong. 2011. Critical roles of RasGRP1 for invariant NKT cell development. *J. Immunol.* 187:4467–4473. http://dx.doi.org/10.4049/jimmunol.1003798

Stritesky, G.L., S.C. Jameson, and K.A. Hogquist. 2012. Selection of self-reactive T cells in the thymus. *Annu. Rev. Immunol.* 30:95–114. http://dx.doi.org/10.1146/annurev-immunol-020711-075035

Verstichel, G., D. Vermijlen, L. Martens, G. Goetgeluk, M. Brouwer, N. Thiault, Y. Van Caeneghem, S. De Munter, K. Weening, S. Bonte, et al. 2017. The checkpoint for agonist selection precedes conventional selection in human thymus. *Sci. Immunol.* 2:eaah4232. http://dx.doi.org/10.1126/sciimmunol.aah4232

Werlen, G., B. Hausmann, and E. Palmer. 2000. A motif in the alphabeta T-cell receptor controls positive selection by modulating ERK activity. *Nature.* 406:422–426. http://dx.doi.org/10.1038/35019094

Werlen, G., B. Hausmann, D. Naeher, and E. Palmer. 2003. Signaling life and death in the thymus: timing is everything. *Science.* 299:1859–1863. http://dx.doi.org/10.1126/science.1067833

Xing, Y., X. Wang, S.C. Jameson, and K.A. Hogquist. 2016. Late stages of T cell maturation in the thymus involve NF-κB and tonic type I interferon signaling. *Nat. Immunol.* 17:565–573. http://dx.doi.org/10.1038/ni.3419

Yu, W., H. Nagaoka, M. Jankovic, Z. Misulovin, H. Suh, A. Rolink, F. Melchers, E. Meffre, and M.C. Nussenzweig. 1999. Continued RAG expression in late stages of B cell development and no apparent re-induction after immunization. *Nature.* 400:682–687. http://dx.doi.org/10.1038/23287

Zabel, B.A., W.W. Agace, J.J. Campbell, H.M. Heath, D. Parent, A.I. Roberts, E.C. Ebert, N. Kassam, S. Qin, M. Zovko, et al. 1999. Human G protein-coupled receptor GPR-9-6/CC chemokine receptor 9 is selectively expressed on intestinal homing T lymphocytes, mucosal lymphocytes, and thymocytes and is required for thymus-expressed chemokine-mediated chemotaxis. *J. Exp. Med.* 190:1241–1256. http://dx.doi.org/10.1084/jem.190.9.1241